

Conceptualizing biogeochemical reactions with an Ohm's law analogy

Tang Jinyun¹, Tang Jinyun¹, Riley William¹, Maschmann Gianna L¹, and Brodie Eoin L¹

¹Lawrence Berkeley National Laboratory

November 16, 2022

Abstract

In studying problems like plant-soil-microbe interactions in environmental biogeochemistry and ecology, one usually has to quantify and model how substrates control the growth of, and interaction among, biological organisms. To address these substrate-consumer relationships, many substrate kinetics and growth rules have been developed, including the famous Monod kinetics for single substrate-based growth, Liebig's law of the minimum for multiple-nutrient co-limited growth, etc. However, the mechanistic basis that leads to these various concepts and mathematical formulations and the implications of their parameters are often quite uncertain. Here we show that an analogy based on Ohm's law in electric circuit theory is able to unify many of these different concepts and mathematical formulations. In this Ohm's law analogy, a resistor is defined by a combination of consumers' and substrates' kinetic traits. In particular, the resistance is equal to the mean first passage time that has been used by renewal theory to derive the Michaelis-Menten kinetics under substrate replete conditions for a single substrate as well as the predation rate of individual organisms. We further show that this analogy leads to important insights on various biogeochemical problems, such as (1) multiple-nutrient co-limited biological growth, (2) denitrification, (3) fermentation under aerobic conditions, (4) metabolic temperature sensitivity, and (5) the accuracy of Monod kinetics for describing bacterial growth. We expect our approach will help both modelers and non-modelers to better understand and formulate hypotheses when studying certain aspects of environmental biogeochemistry and ecology.

24 **Abstract:** In studying problems like plant-soil-microbe interactions in environmental
25 biogeochemistry and ecology, one usually has to quantify and model how substrates control the
26 growth of, and interaction among, biological organisms. To address these substrate-consumer
27 relationships, many substrate kinetics and growth rules have been developed, including the
28 famous Monod kinetics for single substrate-based growth, Liebig's law of the minimum for
29 multiple-nutrient co-limited growth, etc. However, the mechanistic basis that leads to these
30 various concepts and mathematical formulations and the implications of their parameters are
31 often quite uncertain. Here we show that an analogy based on Ohms' law in electric circuit
32 theory is able to unify many of these different concepts and mathematical formulations. In this
33 Ohm's law analogy, a resistor is defined by a combination of consumers' and substrates' kinetic
34 traits. In particular, the resistance is equal to the mean first passage time that has been used by
35 renewal theory to derive the Michaelis-Menten kinetics under substrate replete conditions for a
36 single substrate as well as the predation rate of individual organisms. We further show that this
37 analogy leads to important insights on various biogeochemical problems, such as (1) multiple-
38 nutrient co-limited biological growth, (2) denitrification, (3) fermentation under aerobic
39 conditions, (4) metabolic temperature sensitivity, and (5) the accuracy of Monod kinetics for
40 describing bacterial growth. We expect our approach will help both modelers and non-modelers
41 to better understand and formulate hypotheses when studying certain aspects of environmental
42 biogeochemistry and ecology.

43 **Plain Language Summary**

44 Currently, scientists often use ad-hoc or empirical approaches to conceptualize and formulate
45 biogeochemical processes encountered in environmental sciences. Here we propose that many
46 biogeochemical processes can be coherently conceptualized and formulated using an analogy

47 based on the Ohm's law, a mathematical theory that is widely used to model electric circuits, and
48 also the land-atmosphere exchange of water and energy. We show that this Ohm's law analogy is
49 able to explain observations such as why microbial growth would follow the Monod kinetics,
50 how sometimes fermentation could dominate aerobic respiration when glucose in great supply,
51 how plant and microbes grow under multiple substrates co-limitation, etc. Since this Ohm's law
52 analogy unifies the mathematical foundation of biogeophysics and biogeochemistry, we believe
53 it can potentially lead to more robust land ecosystem models for projecting the climate change.

54 **1. Introduction**

55 In earth system modeling, biogeochemistry strongly affects mass and energy exchanges
56 between ecosystems and the physical climate system [*Heinze et al.*, 2019]. Morphologically,
57 biogeochemistry has three pillars: biology, geophysics, and chemistry. In the context of
58 mathematical modeling, geophysics and chemistry generally have much stronger theoretical
59 foundations than biology [*Brutsaert*, 2005; *Stumm and Morgan*, 1996; *Vallis*, 2006], even though
60 all three are macroscale responses that emerge from atomic interactions, which in an ideal (but
61 impractical) scenario can be predicted by solving the Schrödinger equation of all atoms together
62 (so that arguably they all are subtopics of physics) [*Feynman et al.*, 2011b].

63 In seeking a better understanding of ecological dynamics, e.g., competition and
64 symbiosis, mathematical formulations of the consumer-substrate relationship are essential for
65 both theoretical modeling and interpreting empirical experiments [*Tilman*, 1982]. In the past,
66 three approaches have been used to obtain such relationships. The first approach is by fitting
67 certain empirical response functions to observational data [e.g., *Monod*, 1949]. The second
68 approach is based on an ad-hoc heuristic conceptualization of the problem, e.g., the logistic
69 equation was derived by adding a quadratic term to dissipate the exponential growth of a

70 population when Pierre-Francois Verhulst (1804-1849) was helping his teacher Alphonse
71 Quetelet (1775-1874) to model human population dynamics [*Cramer*, 2002]. The third approach
72 is based on systematic applications of some theory, such as the law of mass action [*Atkins et al.*,
73 2016], statistical mechanics [*Ma*, 1985], and renewal theory [*Doob*, 1948]. Notably, Michaelis-
74 Menten kinetics (and some of its extensions) can be derived by applying any of these theories
75 (see reviews in [*Kooijman*, 1998; *Swenson and Stadie*, 2019; *Tang and Riley*, 2013; 2017]), with
76 the renewal theory even being able to show that Michaelis-Menten kinetics is the statistical mean
77 of the stochastic description of a single enzyme molecule processing the substrate molecules
78 [*English et al.*, 2006; *Reuveni et al.*, 2014].

79 Compared to the empirically-based and ad-hoc approaches, which generally provide
80 limited understanding of the processes implied by the parameters, theory-based approaches have
81 the advantage of linking various related albeit fragmented knowledge (that is abstracted from a
82 much wider range of observations compared to the limited amounts of observational data used by
83 the empirically-based approaches), thereby enabling a deeper understanding of the processes and
84 systems of interest. For instance, when law of mass action is used to derive the Michaelis-
85 Menten kinetics, using the related theory of chemical reaction rates (e.g., Smoluchowski's
86 diffusion model of chemical reaction [*von Smoluchowski*, 1917]), *Tang and Riley* [2019b] were
87 able to upscale the microbially-enabled reactions from one permease to a single bacteria cell and
88 then to a representative soil volume ($\sim O(1 \text{ cm}^3)$), and used the results to explain why substrate
89 affinity parameters are highly variable in soil. Additionally, the theory-based approach has been
90 used to derive the temperature response function of microbial activity [*Ghosh and Dill*, 2010],
91 and to explain why Michaelis-Menten kinetics are more appropriate for microbial uptake of

92 small molecules, while reverse Michaelis-Menten kinetics are more appropriate for enzyme
93 degradation of organic polymer particles [*Tang and Riley, 2019a*].

94 In this paper, we first introduce an analogy that uses the Ohms' law from electric circuit
95 theory to interpret the resource-consumer relationship. Similar analogies have been widely used
96 by land models to represent the physics of land-atmosphere exchanges of water, gases, and
97 energy [e.g., *Lawrence et al., 2019; Riley et al., 2011; Shuttleworth and Wallace, 1985; Wu et*
98 *al., 2009*]. (So that in a certain sense, the Ohm's law is unifying all three aspects of
99 biogeochemistry into physics.) We then exploit this analogy to explain several interesting
100 biogeochemical phenomena that are observed in various context. We conclude the paper with
101 recommendations of other potential applications of this analogy.

102 Although the example problems below are solved with the Ohm's law analogy, we note
103 that they can all be solved using the more accurate Equilibrium Chemistry Approximation (ECA)
104 kinetics [*Tang and Riley, 2013*] or the synthesizing unit plus ECA (SUPECA) kinetics [*Tang and*
105 *Riley, 2017*]. However, the Ohms' law analogy proposed here is more intuitive and can provide
106 an alternative to the ECA and SUPECA kinetics in formulating biogeochemical models.

107 **2 Methods**

108 **2.1 A brief review of Ohm's law and circuit theory**

109 We below briefly review Ohm's law and the theory of series and parallel resistor circuits.
110 More detailed descriptions of circuit theory can be found in *Feynman et al. [2011a]*.

111 Ohm's law describes the relationship between voltage (V), electric current (I), and
112 resistor (r):

$$I = \frac{V}{r}. \tag{1}$$

113 To simplify the presentation, we assume that all variables are properly defined with their
114 international units.

115 For a series concatenation of resistors r_j , application of Ohm's law yields

$$I = \frac{V}{\sum_j r_j}. \quad (2)$$

116 For a parallel concatenation of resistors r_j , application of Ohm's law leads to

$$I = V \left(\sum_j \frac{1}{r_j} \right), \quad (3)$$

117 and the electric current through each resistor is

$$I_j = \frac{V}{r_j}. \quad (4)$$

118 From equations (3) and (4), we can further derive

$$\frac{I_j}{I} = \frac{1}{1 + \left(\sum_{l \neq j} \frac{r_l}{r_j} \right)}, \quad (5)$$

119 which states that when all other resistors are fixed, the fraction of current through r_j increases
120 with decreasing r_j . We will see later that this inference is very useful to explain shifts in
121 metabolic pathways in biological organisms.

122 **2.2. Michaelis-Menten kinetics interpreted with Ohm's law**

123 Michaelis-Menten kinetics represents the single-enzyme catalyzed single-substrate
124 reaction velocity v as

$$v = \frac{v_{max}ES}{K+S}, \quad (6)$$

125 where, in the original application by *Michaelis and Menten* [1913], v_{max} is the maximum
126 specific hydrolysis rate enabled by the invertase and E , S , and K are enzyme concentration,
127 substrate concentration, and half saturation coefficient, respectively. We note that, for enzymes,
128 K also includes contributions from the dissociation process [e.g., *Briggs and Haldane*, 1925].

129 By defining $k_f = v_{max}/K$, equation (6) can be rewritten as

$$v = \frac{E}{\frac{1}{v_{max}} + \frac{K}{v_{max}S}} = \frac{E}{\frac{1}{v_{max}} + \frac{1}{k_f S}}. \quad (7)$$

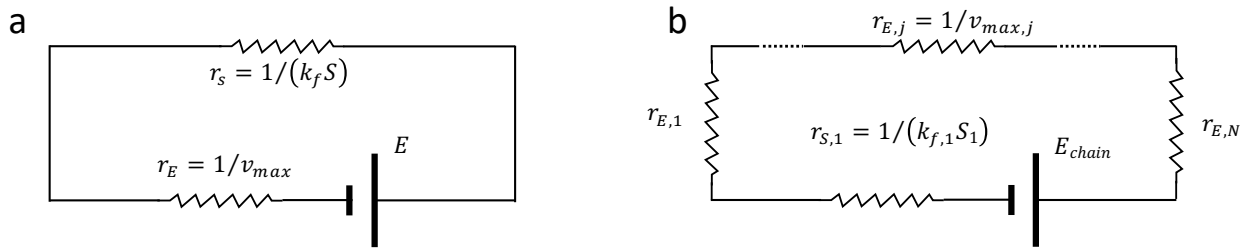
130 We then note that equations (7) and (1) are of the same form. Therefore, for Michaelis-
131 Menten kinetics, if we apply the Ohm's law analogy by regarding E as voltage and v as current,
132 the corresponding resistance is

$$r = \frac{1}{v_{max}} + \frac{1}{k_f S} = r_E + r_S, \quad (8)$$

133 where r_E represents the resistance as an intrinsic property (i.e., a kinetic trait) of the enzyme, and
134 r_S represents the resistance introduced by the effective substrate delivery rate towards the
135 enzyme. Further, r_E and r_S are of the unit of time, where (in the renewal theory [e.g., *Kooijman*,
136 1998]) r_E is the mean time for the enzyme to convert the enzyme-bound substrate molecules into
137 product molecules and r_S is the mean time for the substrate molecules to approach the enzyme
138 molecule and form enzyme-substrate complexes. Together, r is the mean first passage time of
139 the stochastic description of how a single enzyme catalyzes the degradation of the substrate
140 molecules [e.g., *Kooijman*, 1998; *Ninio*, 1987; *Qian*, 2008]. In particular, in many reactions, k_f
141 is approximately proportional to the substrate diffusivity [*Alberty and Hammes*, 1958; *Chou and*
142 *Jiang*, 1974], such that $k_f S$ is the diffusive substrate flux sensed by enzyme molecules. We then
143 observe that r_S increases with the decrease of diffusive substrate flux, which can result from
144 lower substrate concentration, or lower diffusivity (due to tortuosity, adsorption, or lower
145 moisture in porous media like soil).

146 That the resistance r in equation (8) is of the time unit has also motivated some
147 researchers to apply the time budget idea to derive predator-prey relationships [e.g., *Holling*,
148 1959; *Murdoch*, 1973], where r_E is referred as the mean time spent on handling the prey, and r_S

149 is the mean time for the predator to encounter the prey. However, few studies have pointed out
 150 the linkage between the time-budget analysis and Ohm's law, except that, based on a suggestion
 151 by *Thomsen et al.* [1994], *Almeida et al.* [1997] made an analogy of the membrane electron-
 152 transport chain to an electric circuit, and successfully used it to model denitrification. Recently,
 153 this method has been used by *Domingo-Felez and Smets* [2020] to build the Activated Sludge
 154 Model-Electron Competition (ASM-EC) model, which demonstrated the efficacy of this analogy
 155 in constructing robust biogeochemical models. Further, we noticed that the molecular biology of
 156 membrane electron transport chains and redox reactions are quite similar to the working
 157 principles of chemical batteries [*Schmidt-Rohr*, 2018], thereby motivating us to explore more
 158 extensively the applicability of Ohm's law analogy below.



159
 160 Figure 1. **a.** circuit schema for the Michaelis-Menten kinetics; **b.** series resistor-based schema for
 161 an enzyme chain and its reaction on substrate S_1 , where dotted lines indicate multiple resistors
 162 $r_{E,j}$ concatenated in series. Symbols are explained in the main text.

163 In the Ohm's law analogy, kinetic interactions between an enzyme and its substrate
 164 molecules can be summarized as the battery-resistor relationship shown in Figure 1a, where the
 165 battery potential is enzyme concentration E , and the battery's resistance is r_E , while the
 166 appliance (i.e., substrate) has resistance r_s . However, we note that this analogy is accurate only
 167 when the substrate is non-limiting for the enzymes (i.e., when MM kinetics are more appropriate
 168 [*Tang and Riley*, 2019a]). For cases when substrate is limiting, the reverse Michaelis-Menten
 169 kinetics are more appropriate [*Tang*, 2015], and the roles of substrate and enzyme in the analogy

170 are reversed (such as for enzyme hydrolysis of polymeric organic matter; [Tang and Riley,
171 2019a]). (We note that the ECA kinetics are able to more accurately handle the wide range of
172 substrate abundances with respect to enzymes [Tang, 2015].) We next show how the Ohm's law
173 analogy will help us formulate biogeochemical kinetics for various situations.

174 **3. Applications**

175 **3.1 Series resistor circuit-based formulation of chain-like enzyme reactions**

176 Many metabolic pathways consist of a chain of reactions. Such examples include the
177 Calvin-cycle (in photosynthesis), membrane electron transport chain, glycolysis, citric acid
178 cycle, etc., and note that most of these reaction pathways involve cofactors [Madigan *et al.*,
179 2009; Taiz and Zeiger, 2006]. Nonetheless, assuming that at each step the enzyme and its co-
180 factor together form an integrated enzyme unit to process the substrate delivered from a prior
181 step, and the whole chain of enzymatic reactions are in detailed balance (i.e., the whole chain is
182 in steady state without overflow [Cao, 2011], an assumption that is often made in flux balance
183 models [Orth *et al.*, 2010]), we can then use the series circuit analogy to calculate the overall
184 enzyme kinetics straightforwardly. According to the schema for this configuration (Figure 1b),
185 when the whole enzyme chain is taken as a catalysis unit, the abundance of enzyme at the first
186 step represents the voltage of the battery, and the total resistance is

$$r_{chain} = \left(\sum_{j=1}^N r_{E,j} \right) + r_{S,1} = r_E + r_{S,1}, \quad (9)$$

187 where $r_{E,j} = v_{max,j}^{-1}$ such that the first right hand side term is the total resistance represented by
188 the maximum catalysis rate of the overall enzyme chain, and $r_{S,1} = (k_{f,1}S_1)^{-1}$ is the resistance
189 due to the incoming substrate flux to the first enzyme in the chain. For the overall chain, the
190 specific reaction rate for substrate processing is then

$$\frac{v_{chain}}{E_{chain}} = \frac{1}{r_{chain}} = \frac{\left(\sum_{j=1}^N v_{max,j}^{-1}\right)^{-1} S_1}{\frac{K_1}{v_{max,1}\left(\sum_{j=1}^N v_{max,j}^{-1}\right) + S_1}}, \quad (10)$$

191 where $K_1 = v_{max,1}/k_{f,1}$. Equation (10) can be simplified as

$$\frac{v_{chain}}{E_{chain}} = \frac{v_{max,chain} S_1}{K_{chain} + S_1}, \quad (11)$$

192 with

$$v_{max,chain} = \left(\sum_{j=1}^N v_{max,j}^{-1}\right)^{-1} < \min_j\{v_{max,j}\}, \quad (12)$$

193 and

$$K_{chain} = \frac{K_1}{v_{max,1}\left(\sum_{j=1}^N v_{max,j}^{-1}\right)} = \frac{K_1}{1 + \sum_{j=2}^N v_{max,1}/v_{max,j}}. \quad (13)$$

194 From equation (10), we assert that an enzyme chain is equivalent to an enzyme unit with kinetic
 195 traits $v_{max,chain}$ and K_{chain} . Moreover, from equations (12) and (13), we infer that increasing the
 196 chain length decreases the overall reaction rate $v_{max,chain}$ (which is even slower than the
 197 slowest step) and the half saturation coefficient K_{chain} of the enzyme chain.

198 Several interesting inferences can be additionally drawn from equations (9)-(13). First,
 199 the second law of thermodynamics suggests that a thermal engine has higher thermodynamic
 200 efficiency when it runs slower (and the highest efficiency can only be achieved when the system
 201 is in thermodynamic equilibrium, i.e., not running at all [*Salamon et al.*, 2001]). Since a longer
 202 reaction chain slows down the overall transformation rate from a given substrate to its final
 203 product, (as an example,) application of the above equations to electron transport chains leads us
 204 to assert that a longer chain will likely be thermodynamically more efficient (this argument
 205 echoes the Ladder theorem in finite time thermodynamics; [*Salamon et al.*, 2017]). In contrast,
 206 shorter electron transport chains imply faster use of substrates even though they result in less
 207 efficient substrate use. Therefore, the length of electron transport chains can characterize the

208 tradeoff between substrate use rate and substrate use efficiency, an important selection factor for
 209 organisms during their evolution. Indeed, in one chemostat based study, *Chen et al.* [2017] found
 210 that Vibrionales bypass respiratory complex III to consume part of the oxygen using a
 211 cytochrome bd terminal oxidase to speed up growth, but the bioenergetic efficiency becomes
 212 ~32% as compared to ~80% for the longer canonical respiratory chain. Similarly, observations
 213 indicate that the less efficient fermentation pathway which has fewer enzymes involved is faster
 214 than the aerobic respiration pathway that has many more enzymes involved (thus is longer and
 215 more efficient; [Madigan et al., 2009]). We will later (in section 3.5) use the parallel circuit
 216 analogy to explain why such bypassing of more efficient pathways will occur under substrate
 217 abundant conditions.

218 The second inference to be made is about the temperature sensitivity of parameters
 219 $v_{max,chain}$ and K_{chain} . In the simplest one-step case, $v_{max,chain}$ equals $v_{max,1}$, and K_{chain} equals
 220 K_1 . According to transition state theory [e.g., Eyring, 1935], $v_{max,1}$ would have the following
 221 temperature dependence,

$$v_{max,1} = v_{max,1,ref} T \cdot \exp\left(-\frac{\Delta G_1}{RT}\right), \quad (14)$$

222 where $v_{max,1,ref}$ is some reference reaction rate, T is temperature, ΔG_1 is the Gibbs energy of
 223 activation, and R is the universal gas constant. Similarly, for a reaction pathway consisting of a
 224 chain of enzymes, each $v_{max,j}$ will have a temperature dependence similar to that in equation
 225 (14), that is

$$v_{max,j} = v_{max,j,ref} T \cdot \exp\left(-\frac{\Delta G_j}{RT}\right), \quad (15)$$

226 which when entered into equation (12), $v_{max,chain}$ will then be of the form

$$v_{max,chain} = \left[\sum_{j=1}^N \left(v_{max,j,ref}^{-1} \exp\left(\frac{\Delta G_j - \Delta G_1}{RT}\right) \right) \right]^{-1} T \cdot \exp\left(-\frac{\Delta G_1}{RT}\right). \quad (16)$$

227 Therefore, if $(\Delta G_j - \Delta G_1)/(RT) \ll 1$, the temperature dependence of $v_{max,chain}$ will be
228 approximately like that in equation (14).

229 The temperature dependence of K_1 is determined by the temperature dependencies of
230 $v_{max,1}$ and $k_{f,1}$. Inside the microbial cytoplasm and cell membrane (and also for whole microbial
231 cells in most natural environments), $k_{f,1}$ is closely related to diffusivity [*Madigan et al.*, 2009].
232 Thus, according to the Stokes-Einstein equation of diffusivity ($D = (k_B T)/(6\pi\eta a)$, where k_B is
233 the Boltzmann constant, η is the dynamic viscosity, and a is the radius of the spherical particle)
234 [*Feynman et al.*, 2011c], $k_{f,1}$ can be approximated with a linear dependence on temperature
235 divided by the temperature sensitivity of η (which is $\exp(B/(T - T_{VF}))$), where B and T_{VF} are
236 empirical parameters, according to the semi-empirical Vogel-Fulcher-Tamman-Hesse equation
237 [*Garcia-Colin et al.*, 1989]). When the temperature dependence of $k_{f,1}$ is combined with the
238 Eyring-type temperature dependence of $v_{max,1}$, the definition of $K_1 (= v_{max,1}/k_{f,1})$ suggests
239 that its temperature dependence is of the Arrhenius type (because $\exp(B/(T - T_{VF}))$ of the
240 viscosity is very similar to the Arrhenius equation, and the linear temperature dependence of $k_{f,1}$
241 cancels out the linear part of the temperature dependence of $v_{max,1}$). Once again, if
242 $(\Delta G_j - \Delta G_1)/(RT) \ll 1$, K_{chain} will probably have an Arrhenius-type temperature sensitivity as
243 well.

244 When the above inferences are put into equation (11), we can then infer the temperature
245 dependence of v_{chain} . From chemical thermodynamics, the temperature dependence of v_{chain}
246 depends on chemical kinetics (as characterized by the Michaelis-Menten term, i.e., $\frac{v_{max,chain}S_1}{K_{chain}+S_1}$ in
247 this example) and thermodynamics (as a function of the Gibbs free energy) of the enzyme
248 catalyzed reaction. However, because enzymes are proteins, their conformational states are also

249 temperature dependent [Murphy *et al.*, 1990]. Thermodynamically, the undenatured (aka
 250 catalytically active) fraction of an enzyme population of length n_x (as measured by the number
 251 of amino acid residues) can be described as [Murphy *et al.*, 1990]

$$f_{ax} = \frac{1}{1 + \exp\left(\frac{-n_x \Delta G_x}{RT}\right)}, \quad (17)$$

252 where

$$\Delta G_x = \Delta H^* - T \Delta S^* + \Delta C_p [(T - T_H^*) - T \ln(T/T_S^*)], \quad (18)$$

253 and

$$\Delta C_p = -46.0 + 30(1 - 1.54n_x^{-0.268})N_{CH,x}, \quad (19)$$

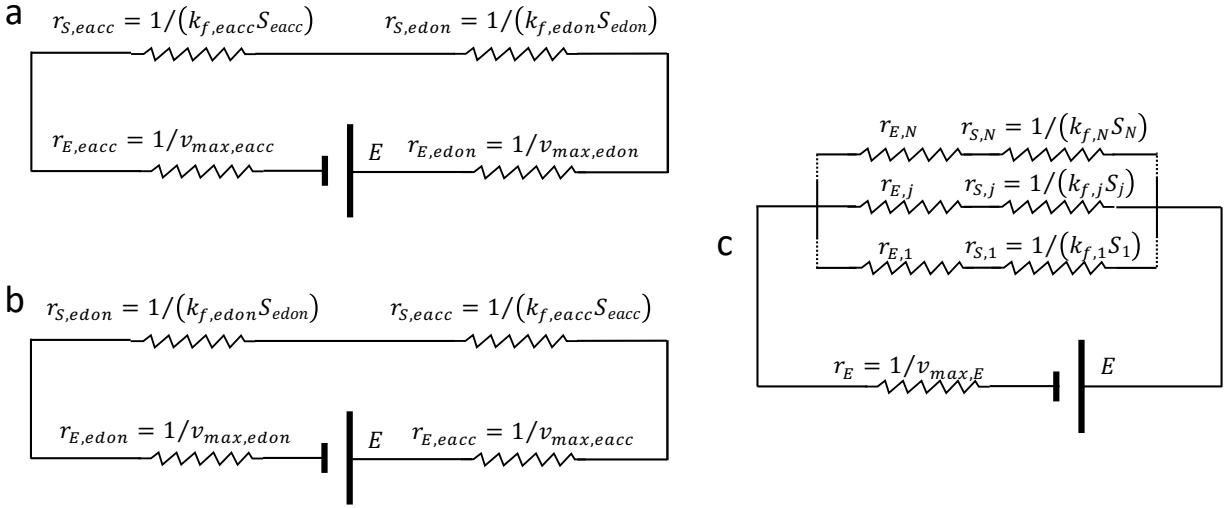
254 with heat capacity ΔC_p defined as the energy required to reorganize the water molecules
 255 surrounding the protein [Ratkowsky *et al.*, 2005]. ΔC_p increases with the non-polar accessible
 256 area of the molecule, as measured by $N_{CH,x}$, the average number of non-polar hydrogen atoms
 257 per amino acid residue. ΔC_p also measures the hydrophobic contribution, with higher values
 258 implying higher hydrophobicity (and notice that greater $N_{CH,x}$ implies higher hydrophobicity).
 259 Other parameters include ΔS^* as the enthalpy change at T_S^* (the convergence temperature for
 260 entropy) and ΔH^* as the enthalpy change at T_H^* (the convergence temperature for enthalpy),
 261 which can be considered to be constant under environmental conditions [e.g., Ratkowsky *et al.*,
 262 2005]. Assuming $N_{CH,x}$ and n_x can be obtained from proteomic data for each type of enzyme
 263 [e.g., Sawle and Ghosh, 2011], we can then calculate $f_{ax,j}$ for all enzymes involved in the chain.
 264 Therefore, putting together the kinetic, thermodynamic, and catalytically active enzyme fraction
 265 functions, we obtain

$$v_{chain} = \frac{v_{max,chain} S}{K_{chain} + S} F_T \prod_j f_{ax,j}, \quad (20)$$

266 where the thermodynamic temperature dependence of the reaction is

$$F_T = 1 - \exp\left(-\frac{\Delta G_{reac}}{RT}\right), \quad (21)$$

267 with ΔG_{reac} being the Gibbs free energy of the overall reaction being catalyzed, which is defined
 268 by the chemical activity of initial substrates and final products [e.g., *Jin and Bethke, 2007*].



269

270 Figure 2. **a.** type-1 circuit schema for redox-type reaction; **b.** type-2 circuit schema for redox-
 271 type reaction; **c.** circuit schema for parallel resistor-based schema for competitive enzymatic
 272 reactions. Type-1 and Type-2 schema are equivalent, and are not differentiated in the Ohm's law
 273 analogy. Symbols are explained in the main text.

274 Unless equation (20) is applied to organisms capable of growing on alternative electron
 275 acceptors or donors, and the system is undergoing fast transition in redox status (e.g., at the depth
 276 of the soil water table), F_T is very close to 1, and can be ignored. Therefore, the temperature
 277 dependence of v_{chain} is dominated by the kinetic term (i.e., that of the Michaelis-Menten term)
 278 and the temperature dependent fraction of active enzymes ($\prod_j f_{ax,j}$). The kinetic term increases
 279 with temperature, while the fraction of active enzymes first increases, then decreases with
 280 temperature. The overall temperature sensitivity of the reaction chain will be of the form
 281 predicted by the macromolecular rate theory (MMRT) (with fine tuning from substrate
 282 availability through the kinetic term which MMRT does not consider) [*Arcus et al., 2016*;
 283 *Schipper et al., 2014*]. Therefore, for a population of cells that are not under substrate limitation

284 and steadily growing (so that one metabolic pathway dominates the metabolism), one should
 285 expect a MMRT type temperature dependence of the metabolic rates. This thus explains why
 286 *Ratkowsky et al.* [2005] was able to use the following equation to model bacterial growth rates
 287 under unlimited substrate supply:

$$g = \frac{cT \exp(-\Delta H_A/RT)}{1 + \exp\left(-\frac{n}{RT}(\Delta H^* - T\Delta S^* + \Delta C_p[(T - T_H^*) - T \ln(T/T_S^*)])\right)} \quad (22)$$

288 where g is growth rate, c is an empirical constant, and ΔH_A is substrate dependent activation
 289 energy. However, unlike it was historically assumed that properties of some single control
 290 enzyme determine the overgrowth [*Johnson and Lewin*, 1946], here n and ΔC_p represent mean
 291 values of protein length and their thermal property, under possible influences from other
 292 molecules, such as phospholipids [e.g., *Mansy and Szostak*, 2008].

293 3.2 Series resistor-based formulation of enzyme catalyzed redox reactions

294 Many biogeochemical processes are of the redox type, including photosynthesis, aerobic
 295 respiration, nitrification, anaerobic denitrification, etc. [*Madigan et al.*, 2009; *Taiz and Zeiger*,
 296 2006]. Basically, enzyme catalyzed redox reactions facilitate electron transfers from electron
 297 donors to electron acceptors. This process can be summarized with the schema Figure 2a that has
 298 one resistor representing electron donors ($r_{S,edon}$), and the other resistor ($r_{S,eacc}$) representing
 299 electron acceptors, with the enzyme being the battery. By applying the Ohm's law analogy, the
 300 reaction rate is

$$v = \frac{E}{r_{eacc} + r_{edon}}, \quad (23)$$

301 where $r_{eacc} = \frac{1}{v_{max,eacc}} + \frac{1}{k_{f,eacc}S_{eacc}}$, and $r_{edon} = \frac{1}{v_{max,edon}} + \frac{1}{k_{f,edon}S_{edon}}$. When the two are
 302 combined, equation (23) can be rewritten as

$$v = \frac{E}{r_E + \frac{1}{k_{f,eacc}S_{eacc}} + \frac{1}{k_{f,edon}S_{edon}}}. \quad (24)$$

303 with $r_E = \frac{1}{v_{max,eacc}} + \frac{1}{v_{max,edon}}$, $r_{S,eacc} = \frac{1}{k_{f,eacc}S_{eacc}}$, and $r_{S,edon} = \frac{1}{k_{f,edon}S_{edon}}$. We note that in
 304 this series resistor-based formulation, the total resistance (or mean first passage time) does not
 305 include the discount resulting from the concurrent binding of electron donors and acceptors to
 306 the enzyme (i.e., configuration Figure 2b is as good as Figure 2a, and they have the same
 307 resistance). However, this discount can be incorporated by renewal theory (or law of mass
 308 action), which leads to the synthesizing unit (SU) model [Kooijman, 1998] below

$$v = \frac{E}{r_E + \frac{1}{k_{f,eacc}S_{eacc}} + \frac{1}{k_{f,edon}S_{edon}} + \frac{1}{k_{f,eacc}S_{eacc} + k_{f,edon}S_{edon}}}. \quad (25)$$

309 Compared to equation (24), the SU model (i.e., equation (25)) is numerically more
 310 accurate (in approximating the law of mass action, the standard method that deals with
 311 biogeochemical reactions [Koudriavstev *et al.*, 2001]). Equations (24) and (25) differ by the
 312 additional term $-1/(k_{f,eacc}S_{eacc} + k_{f,edon}S_{edon})$ that accounts for the co-existence of schemas
 313 in Figure 2a and Figure 2b.

314 Equation (24) was derived as early as in *Alberty* [1953], and is called the additive model.
 315 It was found as the superior formulation to model multiple nutrient limitations of microbial and
 316 plant growth in *O'Neill et al.* [1989] (where electron donors and acceptors are replaced with
 317 complementary nutrients, such as nitrogen and phosphorus). In particular, the additive model
 318 equation (24) can be extended to include arbitrary number of nutrients:

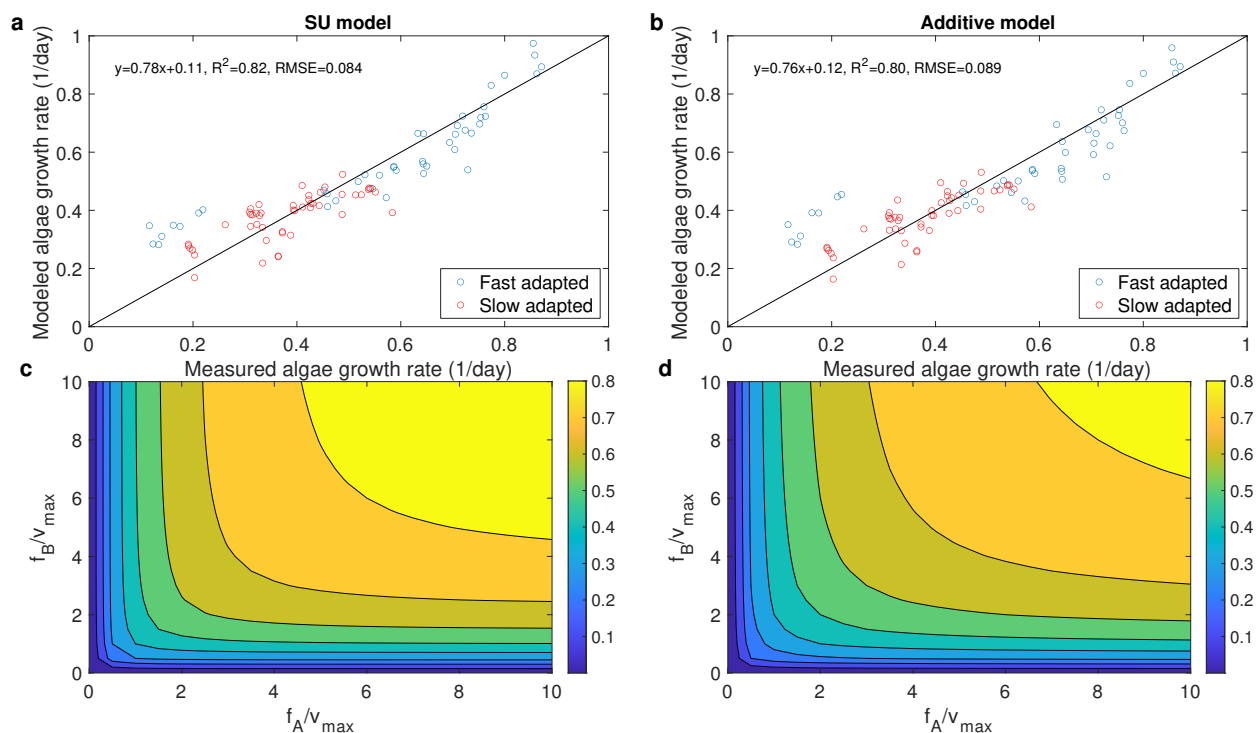
$$v = \frac{E}{r_E + \sum_j \frac{1}{k_{f,j}S_j}}. \quad (26)$$

319 where S_j can be essential nutrients including carbon, nitrogen, phosphorus, potassium,
 320 chloronium, etc. *Smith* [1976; 1979] used equation (26) to model plant growth and microbial

321 growth under carbon, nitrogen, phosphorus, and potassium co-limitation. Based on past
322 successful applications [*Franklin et al.*, 2011; *Kooijman*, 1998], the SU model (i.e., equation
323 (25)) may be argued as mathematically more rigorous than the series resistor-based additive
324 model (i.e., equation (24) or (26)). However, given the usually significant uncertainty of
325 ecological data, the series resistor-based additive model may be equally good. Indeed, when we
326 applied both the SU model and the resistor-based additive model to the measured algal growth
327 rates under various levels of phosphorus and vitamin B₁₂ additions [*Droop*, 1974], both models
328 can be satisfyingly calibrated with respect to the growth data (Figure 3a and b). Further, when
329 the normalized growth rates are contoured as a function of the normalized substrate fluxes, the
330 SU and resistor-based additive models show very similar growth patterns (Figure 3c and d). The
331 SU model and additive model also performed equally well for the plant growth data from *Shaver*
332 *and Melillo* [1984] (Figure 4). Moreover, when the SU model and additive model are used to
333 model aerobic heterotrophic respiration using the parameterization from *Tang and Riley* [2019b],
334 we once again find the two models resulted in very similar goodness of fit with respect to the
335 measurements (Figure 5). These lines of evidence suggest that one can probably use these two
336 models alternatively. In particular, both can be a substitute for Liebig's law of the minimum that
337 is used by most existing biogeochemical models [*Achat et al.*, 2016].

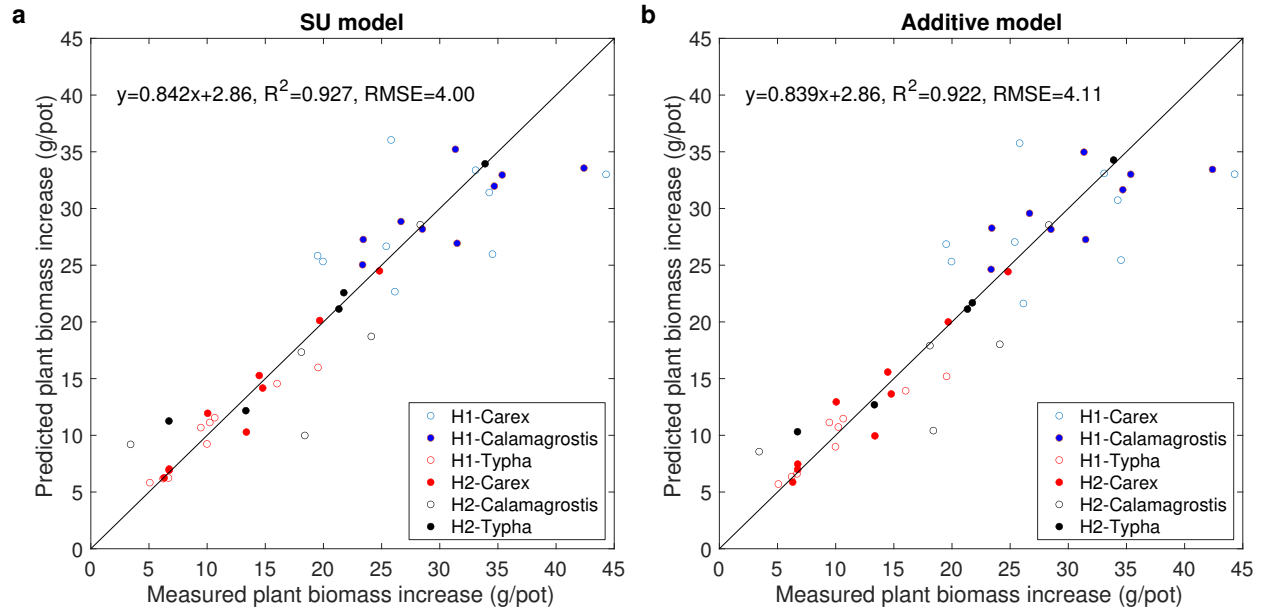
338 Additionally, we note that equation (26) can be extended into a photosynthesis model to
339 replace the Farquhar or Collatz model that is formulated based on Liebig's law of the minimum,
340 which has to arbitrarily smooth the abrupt transitions from one limiting process to another [e.g.,
341 *Collatz et al.*, 1990; *Collatz et al.*, 1992; *Farquhar et al.*, 1980; *Kirschbaum and Farquhar*,
342 1984]. In this context, we contend that it is possible to use the same kinetics to formulate models

343 of plant photosynthesis, microbial substrate dynamics, and biomass growth, a strategy that will
 344 likely enhance the mathematical coherence in modeling plant-soil-microbial interactions.

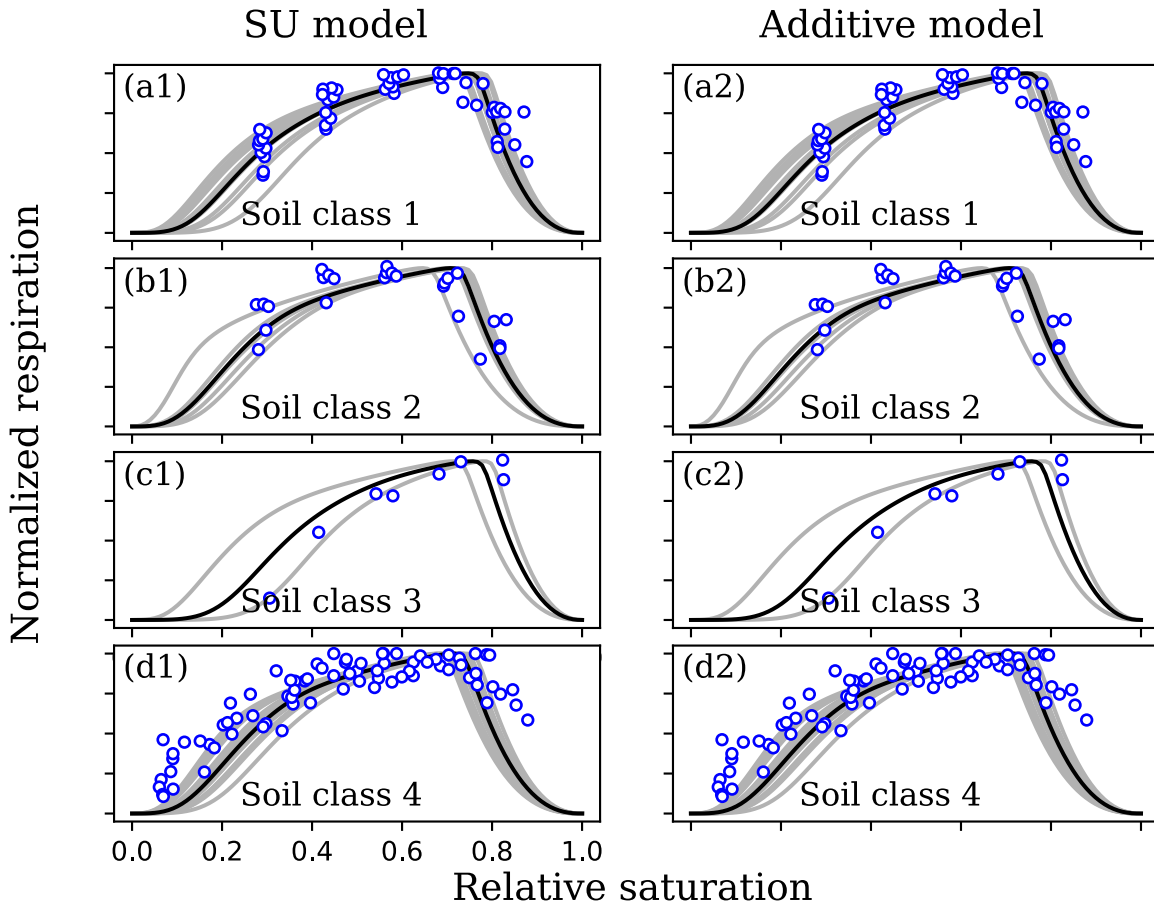


345
 346 Figure 3 **a** comparison of the calibrated synthesizing unit (SU) model prediction for the algal
 347 growth rates data from *Droop* [1974]; **b** same as **a** but from the calibrated resistor-based additive
 348 model; **c** contour of normalized growth rate as a function of normalized fluxes of substrates A
 349 and B for the SU model; **d** same as **c** but for the resistor-based additive model. The additive
 350 model is presented as equation (24), and the SU model is presented as equation (25). Model
 351 parameters are in Table S1 of the supplemental material.

352



353
 354 Figure 4 **a** SU model predicted vs measured plant growth; **b** Additive model predicted vs
 355 measured plant growth. The data is from *Shaver and Melillo* [1984]. Model parameters are in
 356 Table S1 of the supplemental material.

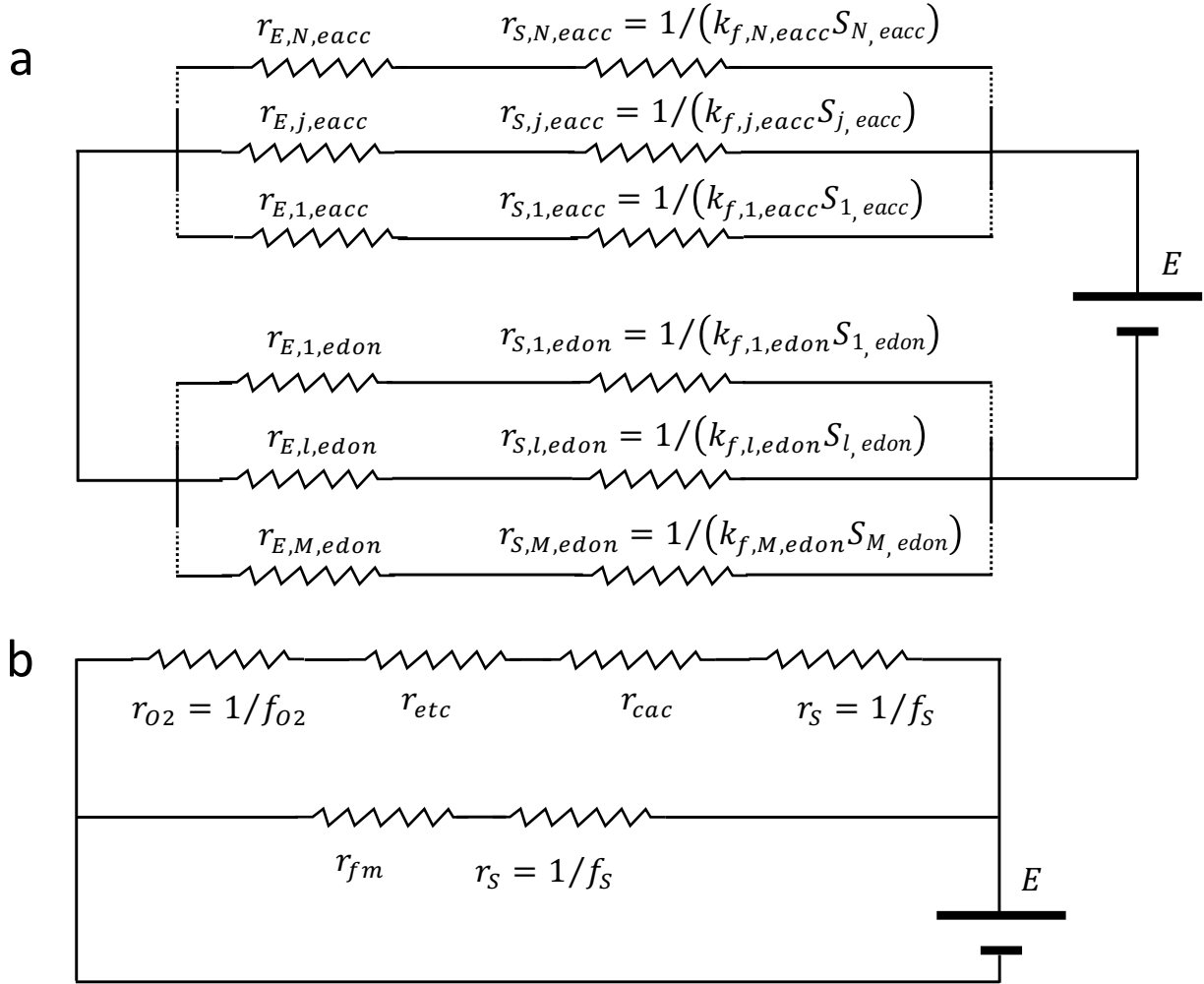


357

358 Figure 5. Left panels are SU model-based prediction of respiration-soil-moisture relationship;
 359 right panels are based on the resistor-based additive model. The two models used identical
 360 parameters, which are detailed in *Tang and Riley* [2019b]. The statistics for model-data fitting (in
 361 terms of linear regression and root mean square error) between two models are identical to 0.01
 362 (see Table S2 of the supplemental material).

363 3.3 Parallel resistor-based formulation of competitive kinetics

364 Many microorganisms can feed on multiple substrates. For example, *E.coli* and yeasts are
 365 able to perform both aerobic and anaerobic respiration [e.g., *Dashko et al.*, 2014; *Uden and*
 366 *Bongaerts*, 1997]. Meanwhile, some enzymes can react on different substrates, e.g., enzyme
 367 ribonuclease is able to degrade various RNA molecules [*Etienne et al.*, 2020]. Thus, we next
 368 show that such problems can be formulated using the parallel circuit (plus one series resistor)
 369 analogy.



370

371 Figure 6. **a** mixed resistor circuit schema for redox reactions with alternative electron donors and
 372 acceptors; **b** circuit schema for the parallel fermentation and aerobic respiration pathways.
 373 Symbols are explained in the main text.

374 We first formulate the competitive Michaelis-Menten kinetics using the schema in Figure

375 2c. For this case, the total resistance is

$$r = r_E + r_S = r_E + \left(\sum_j (r_{E,j} + r_{S,j})^{-1} \right)^{-1}, \quad (27)$$

376 where $r_{S,j}^{-1} = k_{f,j} S_j$, and $r_{E,j}$ is the resistance due to preprocessing of substrate S_j before it is

377 handed to the central enzyme E (i.e., the enzyme that products of all substrates have to pass

378 through), and $r_E = 1/v_{max,E}$ is the resistance due to the maximum substrate processing rate of

379 the central enzyme (which for redox-reactions could be determined by the time spent on
 380 processing the electron donors if S_j here are electron acceptors). If $r_{E,j} = 0$, which is usually
 381 assumed for competitive Michaelis-Menten kinetics, the second term r_s becomes $(\sum_j k_{f,j} S_j)^{-1}$,
 382 and the reaction velocity is

$$v = \frac{E}{r} = \frac{E}{\frac{1}{v_{max}} + (\sum_j k_{f,j} S_j)^{-1}}, \quad (28)$$

383 and the corresponding flux through pathway j is

$$v_j = \frac{v r_s}{r_{s,j}} = v \frac{k_{f,j} S_j}{\sum_l k_{f,l} S_l} = E \cdot \frac{v_{max} S_j / K_j}{1 + \sum_l S_l / K_l}, \quad (29)$$

384 where $K_j = v_{max} / k_{f,j}$. It is easy to see that v_j is the reaction velocity computed from the
 385 competitive Michaelis-Menten kinetics. We note that equation (29) is meaningful only when
 386 pathway j produces new molecules. However, even for inhibitors, whose binding to enzymes
 387 does not produce new molecules, if we regard dissociation as a way of producing new molecules,
 388 then equation (29) is still mathematically meaningful.

389 **3.4 Mixed series and parallel resistor-based formulation of redox reactions of alternative** 390 **electron donors and acceptors**

391 Many microorganisms (such as denitrifying bacteria; e.g., *Robertson and Groffman*
 392 [2015]) are able to grow on different electron donors and acceptors. Such problems can be solved
 393 using the SUPECA kinetics [*Tang and Riley, 2017*]. Below we formulate it using the schema of
 394 mixed series and parallel resistors.

395 Based on the schema in Figure 6a, the total resistance is

$$r = r_{edon} + r_{eacc} = (\sum_l r_{l,edon}^{-1})^{-1} + (\sum_j r_{j,eacc}^{-1})^{-1}, \quad (30)$$

396 where the resistance for electron donors is

$$r_{l,edon} = r_{E,l,eacc} + r_{S,l,eacc} = \frac{1}{v_{max,l,eacc}} + \frac{1}{k_{f,l}S_{l,eacc}}, \quad (31)$$

397 and the resistance for electron acceptors is

$$r_{j,eacc} = r_{E,j,edon} + r_{S,j,edon} = \frac{1}{v_{max,j,edon}} + \frac{1}{k_{f,j,edon}S_{j,edon}}. \quad (32)$$

398 Accordingly, the corresponding reaction flux through electron donor j is

$$v_{j,edon} = \frac{E}{r} \frac{r_{edon}}{r_{j,edon}} = \frac{E}{r_{j,edon}} \frac{r_{edon}}{r_{edon} + r_{eacc}}, \quad (33)$$

399 while the corresponding reaction flux through electron acceptor j is

$$v_{j,eacc} = \frac{E}{r} \frac{r_{eacc}}{r_{j,eacc}} = \frac{E}{r_{j,eacc}} \frac{r_{eacc}}{r_{edon} + r_{eacc}}. \quad (34)$$

400 Now considering an application that involves two electron acceptors, e.g., nitrate and nitrite in
401 denitrification, we have

$$\frac{1}{r_{eacc}} = \frac{1}{r_{NO_3}} + \frac{1}{r_{NO_2}}, \quad (35)$$

402 which when combined with equation (34) leads to

$$v_{NO_3} = \frac{E}{r_{NO_3} + r_{edon} + r_{edon}r_{NO_3}/r_{NO_2}}, \quad (36)$$

403 and

$$v_{NO_2} = \frac{E}{r_{NO_2} + r_{edon} + r_{edon}r_{NO_2}/r_{NO_3}}, \quad (37)$$

404 which are just the equations (10) in *Almeida et al.* [1997] that have been successfully used to fit
405 the measurement of denitrification rates from *Almeida et al.* [1995]. With proper number of
406 resistors, the denitrifier model by *Domingo-Felez and Smets* [2020] can also be easily recovered
407 from equations (30)-(34).

408 **3.5 Other potential applications of the Ohm's law analogy**

409 Besides the applications described above, we below use the Ohm's law analogy to derive
410 some quite interesting results.

411 First, we will explain why fermentation can occur even when there is still oxygen to
 412 support the energetically more efficient aerobic respiration. Such a phenomenon is called the
 413 Warburg effect (i.e., lactate producing aerobic fermentation) in proliferating mammalian cells (a
 414 phenomenon important to the understanding of cancer development), or the Crabtree effect (i.e.,
 415 ethanol fermentation) of unicellular yeast *Sacchamoyces cerevisiae* [e.g., *de Alteriis et al.*, 2018].
 416 *E. coli* have also been observed to shift to the seemingly less efficient yet faster metabolic
 417 pathways under high substrate concentrations [e.g., *Flamholz et al.*, 2013; *Labhsetwar et al.*,
 418 2014]. Depending on the details to be represented, we acknowledge that there are multiple ways
 419 to model such phenomenon even with the circuit analogy. We next present one of these
 420 mathematical explanations to show that, under certain aerobic conditions, high glucose
 421 concentration makes fermentation more favorable.

422 According to the schema in Figure 6b, the specific ATP generation rate from the
 423 fermentation pathway is

$$v_{FM,ATP} = \frac{Y_{FM}}{\frac{1}{f_S} + r_{fm}}, \quad (38)$$

424 where f_S is the incoming flux of pyruvate (produced from glycolysis) sensed by the two
 425 metabolic pathways (which is proportional to the incoming glucose flux sensed by the organism
 426 under steady-state), r_{fm} is the resistance associated with the conversion of pyruvate into
 427 fermentation products (which could be lactate, ethanol, or acetate depending on the organism;
 428 [*Madigan et al.*, 2009]), and Y_{FM} is the ATP yield of fermentation. Similarly, the specific ATP
 429 generation rate from the aerobic respiration pathway is

$$v_{AO,ATP} = \frac{Y_{AO}}{\frac{1}{f_S} + r_{cac} + r_{etc} + \frac{1}{f_{O_2}}}, \quad (39)$$

430 where r_{acc} and r_{etc} are resistance associated with the citric acid cycle, and the electron transport
 431 chain, respectively. f_{O_2} is the incoming oxygen flux, and Y_{AO} is the ATP yield of aerobic
 432 respiration. Because the citric acid cycle involves many more enzyme-catalyzed steps than
 433 fermentation, $r_{cac} > r_{fm}$. Meanwhile, Y_{AO} is about 20 times the value of Y_{fm} [Madigan *et al.*,
 434 2009].

435 In a metabolically active organism, for fermentation to be more favorable than aerobic
 436 respiration, the following condition needs to be satisfied,

$$\frac{Y_{FM}}{Y_{AO}} > \frac{\frac{1}{f_S} + r_{fm}}{\frac{1}{f_S} + r_{cac} + r_{etc} + \frac{1}{f_{O_2}}} > \frac{r_{fm}}{r_{cac} + r_{etc} + \frac{1}{f_{O_2}}}, \quad (40)$$

437 where the term after the second “>” suggests that fermentation is more favorable only when
 438 oxygen is below a certain level of availability (note that f_{O_2} is approximately proportional to
 439 diffusion). When the oxygen availability is sufficiently low, higher substrate concentration (i.e.,
 440 greater f_S) will make fermentation more effective in generating ATP. If we further consider that
 441 the fermentation pathway requires the organism to maintain a much smaller number of enzymes
 442 than required for the aerobic oxidation pathway (which is equivalent to increase the value of
 443 Y_{FM}/Y_{AO} , making the inequality (40) easier to be satisfied), we can expect fermentation to be
 444 preferred for high supply of glucose (i.e., greater f_S) even under certain aerobic conditions. (For
 445 anaerobic condition, f_{O_2} approaches zero, and the inequality (40) is easily satisfied). Given the
 446 significance of this problem in various contexts, including methane and hydrogen dynamics in
 447 environment and industrial biogeochemistry [Lu *et al.*, 2009; Madigan *et al.*, 2009], we expect to
 448 study this problem in a more quantitative and extensive way elsewhere.

449 Another very interesting application is to qualitatively explain why Monod kinetics can
 450 fit the substrate-growth rate relationship of an exponentially growing bacterial population

451 [Monod, 1949]. The argument goes like the following. For an exponentially growing bacterial
452 population, the bacteria proteomes are in steady state. Meanwhile, from the Ohm's law analogy
453 described here, we know that any functioning circuit-network can be equivalently represented by
454 a bulk resistor. Therefore, we contend that however complex the circuit representation of a
455 bacterial metabolism would be, it as a whole can be equivalently represented by a resistor r_E .
456 When this r_E is combined with the resistance associated with the incoming substrate flux (see
457 equation (7)), we say that the bacterial growth would very likely follow the Monod kinetics.
458 However, when the bacteria are in transition from one metabolic state into another, extra
459 resistors are introduced accompanying the change of proteomes, and Monod kinetics will fail for
460 such situations [e.g., Erickson *et al.*, 2017]. This argument also explains why models based on
461 flux balance analysis with proteomic constraints can simulate steadily growing *E. coli* and yeast
462 realistically [Labhsetwar *et al.*, 2014; Labhsetwar *et al.*, 2017].

463 **3.6 Limitations of the Ohm's law analogy**

464 While the Ohm's law analogy can be used to model many challenging biogeochemical
465 processes, it is not appropriate for all types of networks. For instance, it is not able to properly
466 couple two or more consumers (i.e., two or more batteries) within a single circuit network, even
467 though the electric-circuit theory itself does not forbid such a configuration to occur (which can
468 be solved with the Kirchhoff's law of voltage and current [e.g., Feynman *et al.*, 2011a]). Rather,
469 such coupling can only be done by first representing the substrate dynamics of each consumer
470 separately, and then coupling them together by differential equations. Such coupling could be
471 critical when many consumers are competing for a limited substrate, even though none of the
472 consumers is substrate-limited when other consumers are excluded [e.g., Etienne *et al.*, 2020].
473 The equilibrium chemistry approximation (ECA) kinetics [Tang and Riley, 2013] and its progeny

474 SUPECA kinetics [*Tang and Riley, 2017*] are more capable of resolving such situations. In soil
 475 biogeochemistry, one such situation is to model the interaction of a substrate molecule (e.g.,
 476 ammonium, inorganic phosphorus, or dissolved organic carbon) that is simultaneously
 477 undergoing uptake by organisms and adsorption by mineral surfaces. Fortunately, a simple
 478 remedy is possible for the Ohm's law analogy from the ECA kinetics. In the ECA kinetics,
 479 microbial uptake of substrate S under the influence of adsorption by mineral surface M (with
 480 affinity parameter K_M) is

$$F = \frac{v_{max}SB}{K+S+MK/K_M+\alpha B}, \quad (41)$$

481 where K is the half saturation constant for the uptake of S by microbe B in the absence of M , and
 482 αB is the within-population competition effect introduced by ECA. *Tang and Riley [2019a]*
 483 showed that αB is negligible due to the large size contrast between microbes (and likewise fine
 484 roots) and substrate molecules. When αB is ignored, equation (41) becomes

$$F = \frac{B}{\frac{1}{v_{max}} + \frac{1}{k_f S} \left(1 + \frac{M}{K_M}\right)} = \frac{B}{\frac{1}{v_{max}} + \frac{1}{k_f^* S}}, \quad (42)$$

485 with

$$k_f^* = k_f / \left(1 + \frac{M}{K_M}\right). \quad (43)$$

486 Now the Ohm's law analogy will still work if $1/k_f^* S$ is used to defined the substrate dependent
 487 resistance. Moreover, equation (43) suggests that mineral surfaces may slow the microbial
 488 uptake of substrate S by effectively reducing the substrate delivery rate towards the microbes.
 489 However, when the sizes of substrates and competitors are similar (e.g., in some predator-prey
 490 relationships), the Ohm's law analogy will be too cumbersome to apply, and the ECA or
 491 SUPECA kinetics should be used. Nonetheless, it will be very interesting and helpful to

492 construct and compare models for the same system using both the Ohm's law analogy and ECA
493 (or SUPECA) kinetics.

494 **4 Conclusions**

495 By applying the mathematical similarity between the Ohm's law and Michaelis-Menten
496 kinetics, we show that the electric circuit analogy can be used to derive many interesting results
497 of biogeochemical kinetics. We show this approach reproduces many successful applications in
498 the literature, including aerobic heterotrophic respiration, multi-nutrient co-limited microbial
499 (and plant) growth, denitrification dynamics, etc. This approach also sheds new insights on the
500 Warburg and Crabtree effect in prokaryotes and eukaryotes, and conceptually explains why the
501 Monod relationship accurately represents the kinetics of steadily-growing bacterial populations,
502 and why flux balance modeling with proteomic constraints is able to accurately model microbial
503 growth. Based on these results, we expect that the Ohm's law analogy will help build a unified
504 kinetic modelling framework of microbial and plant biogeochemistry to make more robust
505 predictions.

506 **Data Availability Statement**

507 Data is available through *Shaver and Melillo* [1984], *Droop* [1974], *Franzluebbers* [1999], and
508 *Doran et al.* [1990].

509 **Acknowledgement**

510 This research was supported by the Director, Office of Science, Office of Biological and
511 Environmental Research of the US Department of Energy under contract no. DE-AC02-
512 05CH11231 as part of the Next Generation Ecosystem Experiment-Arctic project for JYT and
513 WJR and the TES Soil Warming SFA for WJR and. GLM was supported by funding from the
514 Department of Energy, Office of Biological and Environmental Research, Genomic Sciences

515 Program through the LLNL Microbes Persist Science Focus Area. ELB was supported by
516 funding from the Department of Energy, Office of Biological and Environmental Research,
517 Subsurface Biogeochemical Research Program through the LBNL Watershed Function Science
518 Focus Area. Financial support does not constitute an endorsement by the Department of Energy
519 of the views expressed in this study. The authors declare no conflicts of interest.

520 **Author contributions**

521 JYT conceived the idea and did the analysis; JYT, WJR, GLM and ELB discussed the analysis
522 and wrote the paper.

523

524 **References**

525 Achat, D. L., L. Augusto, A. Gallet-Budynek, and D. Loustau (2016), Future challenges in
526 coupled C-N-P cycle models for terrestrial ecosystems under global change: a review,
527 *Biogeochemistry*, 131(1-2), 173-202, doi:10.1007/s10533-016-0274-9.

528 Alberty, R. A. (1953), The relationship between Michaelis constants, maximum velocities and
529 the equilibrium constant for an enzyme-catalyzed reaction, *J Am Chem Soc*, 75(8), 1928-1932,
530 doi:10.1021/ja01104a045.

531 Alberty, R. A., and G. G. Hammes (1958), Application of the theory of diffusion-controlled
532 reactions to enzyme kinetics, *J Phys Chem-U.S.*, 62(2), 154-159, doi:10.1021/j150560a005.

533 Almeida, J. S., M. A. M. Reis, and M. J. T. Carrondo (1995), Competition between nitrate and
534 nitrite reduction in denitrification by *pseudomonas-fluorescens*, *Biotechnol Bioeng*, 46(5), 476-
535 484, doi:10.1002/bit.260460512.

536 Almeida, J. S., M. A. M. Reis, and M. J. T. Carrondo (1997), A unifying kinetic model of
537 denitrification, *J Theor Biol*, 186(2), 241-249, doi:10.1006/jtbi.1996.0352.

538 Arcus, V. L., E. J. Prentice, J. K. Hobbs, A. J. Mulholland, M. W. Van der Kamp, C. R. Pudney,
539 E. J. Parker, and L. A. Schipper (2016), On the temperature dependence of enzyme-catalyzed
540 rates, *Biochemistry-Us*, 55(12), 1681-1688, doi:10.1021/acs.biochem.5b01094.

541 Atkins, P., L. Jones, and L. Laverman (2016), *Chemical Principles: The Quest for Insight*,
542 Seventh ed., W.H. Freeman.

543 Briggs, G. E., and J. B. S. Haldane (1925), A note on the kinetics of enzyme action., *Biochem J*,
544 19(2), 338-339, doi:10.1042/bj0190338.

545 Brutsaert, W. (2005), *Hydrology: An Introduction*, Cambridge University Press.

546 Cao, J. S. (2011), Michaelis-Menten equation and detailed balance in enzymatic networks, *J*
547 *Phys Chem B*, 115(18), 5493-5498, doi:10.1021/jp110924w.

548 Chen, J. W., et al. (2017), Impacts of chemical gradients on microbial community structure, *Isme*
549 *J*, 11(4), 920-931, doi:10.1038/ismej.2016.175.

550 Chou, K. C., and S. P. Jiang (1974), Studies on the rate of diffusion-controlled reactions of
551 enzymes: spatial factor and force field factor, *Scientia Sinica*, XVII(5), doi:10.1360/ya1974-17-5-
552 664.

553 Collatz, G. J., J. A. Berry, G. D. Farquhar, and J. Pierce (1990), The relationship between the
554 rubisco reaction-mechanism and models of photosynthesis, *Plant Cell Environ*, 13(3), 219-225,
555 doi:10.1111/j.1365-3040.1990.tb01306.x.

556 Collatz, G. J., M. Ribas-Carbo, and J. A. Berry (1992), Coupled photosynthesis-stomatal
557 conductance model for leaves of C4 plants, *Aust J Plant Physiol*, 19(5), 519-538,
558 doi:10.1071/Pp9920519.

559 Cramer, J. S. (2002), *The origins of logistic regression Rep.*, University of Amsterdam and
560 Tinbergen Institute.

561 Dashko, S., N. Zhou, C. Compagno, and J. Piskur (2014), Why, when, and how did yeast evolve
562 alcoholic fermentation?, *Fems Yeast Res*, *14*(6), 826-832, doi:10.1111/1567-1364.12161.

563 de Alteriis, E., F. Carteni, P. Parascandola, J. Serpa, and S. Mazzoleni (2018), Revisiting the
564 Crabtree/Warburg effect in a dynamic perspective: a fitness advantage against sugar-induced cell
565 death, *Cell Cycle*, *17*(6), 688-701, doi:10.1080/15384101.2018.1442622.

566 Domingo-Felez, C., and B. F. Smets (2020), Modeling denitrification as an electric circuit
567 accurately captures electron competition between individual reductive steps: The activated
568 sludge model-electron competition model, *Environ Sci Technol*, *54*(12), 7330-7338,
569 doi:10.1021/acs.est.0c01095.

570 Doob, J. L. (1948), Renewal theory from the point of view of the theory of probability, *T Am*
571 *Math Soc*, *63*(May), 422-438, doi:10.2307/1990567.

572 Doran, J. W., L. N. Mielke, and J. F. Power (1990), Microbial activity as regulated by soil water-
573 filled pore space, in *International Society of Soil Science*, edited.

574 Droop, M. R. (1974), Nutrient status of algal cells in continuous culture, *J Mar Biol Assoc Uk*,
575 *54*(4), 825-855, doi:10.1017/S002531540005760x.

576 English, B. P., W. Min, A. M. van Oijen, K. T. Lee, G. B. Luo, H. Y. Sun, B. J. Cherayil, S. C.
577 Kou, and X. S. Xie (2006), Ever-fluctuating single enzyme molecules: Michaelis-Menten
578 equation revisited, *Nat Chem Biol*, *2*(2), 87-94, doi:10.1038/nchembio759.

579 Erickson, D. W., S. J. Schink, V. Patsalo, J. R. Williamson, U. Gerland, and T. Hwa (2017), A
580 global resource allocation strategy governs growth transition kinetics of *Escherichia coli*, *Nature*,
581 *551*(7678), 119-123, doi:10.1038/nature24299.

582 Etienne, T. A., M. Coccagn-Bousquet, and D. Ropers (2020), Competitive effects in bacterial
583 mRNA decay, *J Theor Biol*, *504*, doi:ARTN 110333 10.1016/j.jtbi.2020.110333.

584 Eyring, H. (1935), The activated complex and the absolute rate of chemical reactions, *Chem Rev*,
585 *17*(1), 65-77, doi:10.1021/cr60056a006.

586 Farquhar, G. D., S. V. Caemmerer, and J. A. Berry (1980), A biochemical-model of
587 photosynthetic CO₂ assimilation in leaves of C₃ species, *Planta*, *149*(1), 78-90,
588 doi:10.1007/Bf00386231.

589 Feynman, R. P., R. B. Leighton, and M. Sands (2011a), *The Feynman Lectures on Physics, Vol*
590 *II: Mainly Electromagnetism and Matter*, The New Millennium Edition ed., Basic Books; New
591 Millennium ed. Edition.

592 Feynman, R. P., R. B. Leighton, and M. Sands (2011b), *The Feynman Lectures on Physics, Vol*
593 *III: Quantum Mechanics*, The New Millennium Edition ed., Basic Books; New Millennium ed.
594 Edition.

595 Feynman, R. P., R. B. Leighton, and M. Sands (2011c), *The Feynman Lectures on Physics, Vol.*
596 *I: Mainly Mechanics, Radiation, and Heat*, The New Millennium Edition ed., Basic Books; New
597 Millennium ed. Edition.

598 Flamholz, A., E. Noor, A. Bar-Even, W. Liebermeister, and R. Milo (2013), Glycolytic strategy
599 as a tradeoff between energy yield and protein cost, *P Natl Acad Sci USA*, *110*(24), 10039-
600 10044, doi:10.1073/pnas.1215283110.

601 Franklin, O., E. K. Hall, C. Kaiser, T. J. Battin, and A. Richter (2011), Optimization of biomass
602 composition explains microbial growth-stoichiometry relationships, *Am Nat*, *177*(2), E29-E42,
603 doi:10.1086/657684.

604 Franzluebbers, A. J. (1999), Microbial activity in response to water-filled pore space of variably
605 eroded southern Piedmont soils, *Appl Soil Ecol*, *11*(1), 91-101, doi:Doi 10.1016/S0929-
606 1393(98)00128-0.

607 Garcia-Colin, L. S., L. F. del Castillo, and P. Goldstein (1989), Theoretical Basis for the Vogel-
608 Fulcher-Tammann Equation, *Phys Rev B*, 40(10), 7040-7044, doi:10.1103/PhysRevB.40.7040.

609 Ghosh, K., and K. Dill (2010), Cellular proteomes have broad distributions of protein stability,
610 *Biophys J*, 99(12), 3996-4002, doi:10.1016/j.bpj.2010.10.036.

611 Heinze, C., et al. (2019), ESD Reviews: Climate feedbacks in the Earth system and prospects for
612 their evaluation, *Earth Syst Dynam*, 10(3), 379-452, doi:10.5194/esd-10-379-2019.

613 Holling, C. S. (1959), Some characteristics of simple types of predation and parasitism, *The*
614 *Canadian Entomologist*, XCI(7), 385-398.

615 Jin, Q., and C. M. Bethke (2007), The thermodynamics and kinetics of microbial metabolism,
616 *Am J Sci*, 307(4), 643-677, doi:10.2475/04.2007.01.

617 Johnson, F. H., and I. Lewin (1946), The growth rate of E-Coli in relation to temperature,
618 quinine and coenzyme, *J Cell Compar Physl*, 28(1), 47-75, doi:10.1002/jcp.1030280104.

619 Kirschbaum, M. U. F., and G. D. Farquhar (1984), Temperature-dependence of whole-leaf
620 photosynthesis in Eucalyptus-pauciflora Sieb ex Spreng, *Aust J Plant Physiol*, 11(6), 519-538,
621 doi:10.1071/Pp9840519.

622 Kooijman, S. A. L. M. (1998), The Synthesizing Unit as model for the stoichiometric fusion and
623 branching of metabolic fluxes, *Biophys Chem*, 73(1-2), 179-188, doi:10.1016/S0301-
624 4622(98)00162-8.

625 Koudriavstev, A. B., R. F. Jameson, and W. Linert (2001), *The law of mass action*, Springer,
626 Berlin Heidelberg, doi:10.1007/978-3-642-56770-4.

627 Labhsetwar, P., J. A. Cole, E. Roberts, N. D. Price, and Z. A. Luthey-Schulten (2014),
628 Heterogeneity in protein expression induces metabolic variability in a modeled Escherichia coli

629 population (vol 110, pg 14006, 2013), *P Natl Acad Sci USA*, *111*(2), 876-876,
630 doi:10.1073/pnas.1323512111.

631 Labhsetwar, P., M. C. R. Melo, J. A. Cole, and Z. Luthey-Schulten (2017), Population FBA
632 predicts metabolic phenotypes in yeast, *Plos Comput Biol*, *13*(9), doi:ARTN e1005728
633 10.1371/journal.pcbi.1005728.

634 Lawrence, D. M., et al. (2019), The Community Land Model Version 5: Description of new
635 features, benchmarking, and impact of forcing uncertainty, *J Adv Model Earth Sy*, *11*(12), 4245-
636 4287, doi:10.1029/2018ms001583.

637 Lu, Y., Q. H. Lai, C. Zhang, H. X. Zhao, K. Ma, X. B. Zhao, H. Z. Chen, D. H. Liu, and X. H.
638 Xing (2009), Characteristics of hydrogen and methane production from cornstalks by an
639 augmented two- or three-stage anaerobic fermentation process, *Bioresource Technol*, *100*(12),
640 2889-2895, doi:10.1016/j.biortech.2009.01.023.

641 Ma, S.-K. (1985), *Statistical Mechanics*, Wspsc.

642 Madigan, M. T., J. M. Martinko, P. V. Dunlap, and D. P. Clark (2009), *Brock biology of*
643 *microorganisms, twelfth edition*, Pearson Education, Inc. , 1301 Sansome Street, San Francisco,
644 CA 94111.

645 Mansy, S. S., and J. W. Szostak (2008), Thermostability of model protocell membranes, *P Natl*
646 *Acad Sci USA*, *105*(36), 13351-13355, doi:10.1073/pnas.0805086105.

647 Michaelis, L., and M. L. Menten (1913), The kinetics of the inversion effect, *Biochem. Z.*, *49*,
648 333-369.

649 Monod, J. (1949), The growth of bacterial cultures, *Annu Rev Microbiol*, *3*, 371-394,
650 doi:10.1146/annurev.mi.03.100149.002103.

651 Murdoch, W. W. (1973), Functional response of predators, *J Appl Ecol*, *10*(1), 335-342.

652 Murphy, K. P., P. L. Privalov, and S. J. Gill (1990), Common features of protein unfolding and
653 dissolution of hydrophobic compounds, *Science*, 247(4942), 559-561,
654 doi:10.1126/science.2300815.

655 Ninio, J. (1987), Alternative to the steady-state method - Derivation of reaction-rates from 1st-
656 passage times and pathway probabilities, *P Natl Acad Sci USA*, 84(3), 663-667,
657 doi:10.1073/pnas.84.3.663.

658 O'Neill, R. V., D. L. Deangelis, J. J. Pastor, B. J. Jackson, and W. M. Post (1989), Multiple
659 nutrient limitations in ecological models, *Ecol Model*, 46(3-4), 147-163, doi:10.1016/0304-
660 3800(89)90015-X.

661 Orth, J. D., I. Thiele, and B. O. Palsson (2010), What is flux balance analysis?, *Nat Biotechnol*,
662 28(3), 245-248, doi:10.1038/nbt.1614.

663 Qian, H. (2008), Cooperativity and specificity in enzyme kinetics: A single-molecule time-based
664 perspective, *Biophys J*, 95(1), 10-17, doi:10.1529/biophysj.108.131771.

665 Ratkowsky, D. A., J. Olley, and T. Ross (2005), Unifying temperature effects on the growth rate
666 of bacteria and the stability of globular proteins, *J Theor Biol*, 233(3), 351-362,
667 doi:10.1016/j.jtbi.2004.10.016.

668 Reuveni, S., M. Urbakh, and J. Klafter (2014), Role of substrate unbinding in Michaelis-Menten
669 enzymatic reactions, *P Natl Acad Sci USA*, 111(12), 4391-4396, doi:10.1073/pnas.1318122111.

670 Riley, W. J., Z. M. Subin, D. M. Lawrence, S. C. Swenson, M. S. Torn, L. Meng, N. M.
671 Mahowald, and P. Hess (2011), Barriers to predicting changes in global terrestrial methane
672 fluxes: analyses using CLM4Me, a methane biogeochemistry model integrated in CESM,
673 *Biogeosciences*, 8(7), 1925-1953, doi:10.5194/bg-8-1925-2011.

674 Robertson, G. P., and P. M. Groffman (2015), Nitrogen transformations, in *Soil microbiology,*
675 *ecology and biochemistry*, edited by E. A. Paul, pp. 421-446, Academic Press, Burlington,
676 Massachusetts, USA.

677 Salamon, P., K. H. Hoffmann, S. Schubert, R. S. Berry, and B. Andresen (2001), What
678 conditions make minimum entropy production equivalent to maximum power production?, *J*
679 *Non-Equil Thermody*, 26(1), 73-83, doi:Doi 10.1515/Jnetdy.2001.006.

680 Salamon, P., T. N. F. Roach, and F. L. Rohwer (2017), The ladder theorem, paper presented at
681 14th Joint European Thermodynamics Conference, Budapest, May 21-25.

682 Sawle, L., and K. Ghosh (2011), How do thermophilic proteins and proteomes withstand high
683 temperature?, *Biophys J*, 101(1), 217-227, doi:10.1016/j.bpj.2011.05.059.

684 Schipper, L. A., J. K. Hobbs, S. Rutledge, and V. L. Arcus (2014), Thermodynamic theory
685 explains the temperature optima of soil microbial processes and high Q(10) values at low
686 temperatures, *Global Change Biol*, 20(11), 3578-3586, doi:10.1111/gcb.12596.

687 Schmidt-Rohr, K. (2018), How batteries store and release energy: explaining basic
688 electrochemistry, *J Chem Educ*, 95(10), 1801-1810, doi:10.1021/acs.jchemed.8b00479.

689 Shaver, G. R., and J. M. Melillo (1984), Nutrient budgets of marsh plants - efficiency concepts
690 and relation to availability, *Ecology*, 65(5), 1491-1510, doi:10.2307/1939129.

691 Shuttleworth, W. J., and J. S. Wallace (1985), Evaporation from sparse crops - an energy
692 combination theory, *Q J Roy Meteor Soc*, 111(469), 839-855, doi:10.1256/smsqj.46909.

693 Smith, O. L. (1976), Nitrogen, phosphorus, and potassium utilization in plant-soil system -
694 analytical model, *Soil Sci Soc Am J*, 40(5), 704-714,
695 doi:10.2136/sssaj1976.03615995004000050029x.

696 Smith, O. L. (1979), Application of a model of the decomposition of soil organic-matter, *Soil*
697 *Biol Biochem*, 11(6), 607-618, doi:10.1016/0038-0717(79)90028-2.

698 Stumm, W., and J. J. Morgan (1996), *Aquatic chemistry: chemical equilibria and rates in natural*
699 *waters*, Wiley.

700 Swenson, H., and N. P. Stadie (2019), Langmuir's theory of adsorption: a centennial review,
701 *Langmuir*, 35(16), 5409-5426, doi:10.1021/acs.langmuir.9b00154.

702 Taiz, L., and E. Zeiger (2006), *Plant physiology, 4th edn*, Sinauer Associates, Inc., Sunderland,
703 MA 01375 USA.

704 Tang, J. Y. (2015), On the relationships between the Michaelis-Menten kinetics, reverse
705 Michaelis-Menten kinetics, equilibrium chemistry approximation kinetics, and quadratic
706 kinetics, *Geosci Model Dev*, 8(12), 3823-3835, doi:10.5194/gmd-8-3823-2015.

707 Tang, J. Y., and W. J. Riley (2013), A total quasi-steady-state formulation of substrate uptake
708 kinetics in complex networks and an example application to microbial litter decomposition,
709 *Biogeosciences*, 10(12), 8329-8351, doi:10.5194/bg-10-8329-2013.

710 Tang, J. Y., and W. J. Riley (2017), SUPECA kinetics for scaling redox reactions in networks of
711 mixed substrates and consumers and an example application to aerobic soil respiration, *Geosci*
712 *Model Dev*, 10(9), 3277-3295, doi:10.5194/gmd-10-3277-2017.

713 Tang, J. Y., and W. J. Riley (2019a), Competitor and substrate sizes and diffusion together
714 define enzymatic depolymerization and microbial substrate uptake rates, *Soil Biol Biochem*, 139,
715 doi:ARTN 107624 10.1016/j.soilbio.2019.107624.

716 Tang, J. Y., and W. J. Riley (2019b), A theory of effective microbial substrate affinity
717 parameters in variably saturated soils and an example application to aerobic soil heterotrophic
718 respiration, *J Geophys Res-Biogeophys*, 124(4), 918-940, doi:10.1029/2018jg004779.

719 Thomsen, J. K., T. Geest, and R. P. Cox (1994), Mass-spectrometric studies of the effect of pH
720 on the accumulation of intermediates in denitrification by paracoccus-denitrificans, *Appl Environ*
721 *Microb*, 60(2), 536-541, doi:10.1128/Aem.60.2.536-541.1994.

722 Tilman, D. (1982), *Resource competition and community structure*, 1st ed., 296 pp., Princeton
723 University Press.

724 Uden, G., and J. Bongaerts (1997), Alternative respiratory pathways of Escherichia coli:
725 Energetics and transcriptional regulation in response to electron acceptors, *Bba-Bioenergetics*,
726 1320(3), 217-234, doi:10.1016/S0005-2728(97)00034-0.

727 Vallis, G. K. (2006), *Atmospheric and Oceanic Fluid Dynamics: Fundamentals and Large-scale*
728 *Circulation*, 1 ed., Cambridge University Press.

729 von Smoluchowski, M. (1917), Versuch einer mathematischen theorie der koagulationkinetik
730 kolloider loesungen., *Z Phys Chem*, 92, 129–132.

731 Wu, Y. H., J. Walker, D. Schwede, C. Peters-Lidard, R. Dennis, and W. Robarge (2009), A new
732 model of bi-directional ammonia exchange between the atmosphere and biosphere: Ammonia
733 stomatal compensation point, *Agr Forest Meteorol*, 149(2), 263-280,
734 doi:10.1016/j.agrformet.2008.08.012.

735